

Article

Structure and Spin State of Iron(II) Assembled Complexes Using 9,10-Bis(4-pyridyl)anthracene as Bridging Ligand

Saki Iwai ¹, Keisuke Yoshinami ¹ and Satoru Nakashima ^{1,2,*}

¹ Graduate School of Science, Hiroshima University, Higashi-Hiroshima 739-8526, Japan; m173497@hiroshima-u.ac.jp (S.I.); m165715@hiroshima-u.ac.jp (K.Y.)

² Natural Science Center for Basic Research and Development, Hiroshima University, Higashi-Hiroshima 739-8526, Japan

* Correspondence: snaka@hiroshima-u.ac.jp; Tel.: +81-82-424-6291

Received: 31 July 2017; Accepted: 7 September 2017; Published: 12 September 2017

Abstract: Assembled complexes, $[\text{Fe}(\text{NCX})_2(\text{bpanth})_2]_n$ ($X = \text{S}, \text{Se}, \text{BH}_3$; $\text{bpanth} = 9,10\text{-bis}(4\text{-pyridyl})\text{anthracene}$), were synthesized. The iron for the three complexes was in temperature-independent high spin state by ^{57}Fe Mössbauer spectroscopy and magnetic susceptibility measurement. X-ray structural analysis revealed the interpenetrated structure of $[\text{Fe}(\text{NCS})_2(\text{bpanth})_2]_n$. In the local structure around the iron atom, the coordinated pyridine planes were shown to be a parallel type, which is in accordance with the results investigated by density functional theory (DFT) calculation. This complex ($X = \text{S}$) has $\text{CH}-\pi$ interactions between the H atom of coordinated pyridine and the neighboring anthracene of the other 2D grid. It was suggested that the interpenetrated structure was supported by the stabilization of $\text{CH}-\pi$ interaction, and this intermolecular interaction forced the relatively unstable parallel structure. That is, the unstable local structure is compensated by the stabilization due to intermolecular interaction, which controlled the spin state as high spin state.

Keywords: assembled complex; Mössbauer spectroscopy; spin crossover; intermolecular interaction controlling local structure

1. Introduction

Iron(II) octahedral assembled complexes can take two spin states (high spin (HS); $S = 2$ and low spin (LS); $S = 0$) in intermediate ligand field [1]. They may show a spin-crossover (SCO) phenomenon between HS state and LS state by several external field stimuli, such as temperature, pressure, and light-illumination. Assembled complexes have an important position in the spin-crossover chemistry [2,3], because they have a variety of structures and the spin state is sometimes controlled by the adsorption/desorption of guest molecules. Reference [4] provides a theoretical review. We have studied iron(II) assembled complexes using various bipyridine-type ligands [5,6]. The change of complex structure and the intermolecular interaction were predicted to influence the SCO phenomenon. The SCO behavior of iron(II) assembled complexes is related to the dihedral angle of pyridine ligands to $\text{Fe}-\text{NCX}$. The SCO appears when the local structure is propeller-type; on the other hand, SCO does not occur when the local structure is parallel or distorted propeller-type, which was demonstrated by density functional theory (DFT) calculation [7,8]. There is also a possibility that the weak π -accepter property of pyridine affects the spin state depending on the local structure around iron atom.

The iron(II) complex $[\text{Fe}(\text{NCX})_2(\text{bpb})_2]_n$ ($X = \text{BH}_3$; $\text{bpb} = 1,4\text{-bis}(4\text{-pyridyl})\text{benzene}$) [9] shows SCO phenomenon. We introduced a methyl substituent to the benzene ring of bpb

(DMBPB = 1,4-dimethyl-2,5-bis(4-pyridyl)benzene) to control the dihedral angle between benzene and pyridine in the bridging ligand [10]. We expected that such change would affect the coordination angle of pyridine to Fe–NCX. Complexes of Ni and Cu using 9,10-bis(4-pyridyl)anthracene (bpanth) including guest molecules have some intermolecular interactions through π electrons [11,12]. In the present study, iron(II) assembled complexes were synthesized using bpanth which has many π -electrons on the bridging ligand. We expected to reveal the relation between intermolecular interactions (π – π or CH– π) and SCO phenomenon.

2. Results

2.1. ^{57}Fe Mössbauer Spectroscopy

The ^{57}Fe Mössbauer spectra of complexes [Fe(NCX)₂(bpanth)₂] (**1** (X = S), **2** (X = Se) and **3** (X = BH₃)) at 78 and 298 K are shown in Figure 1. All spectra showed doublet peaks. The values of isomer shift (I.S.) and quadrupole splitting (Q.S.) are summarized in Table 1. All values of I.S. are close to 1.00 mm·s^{−1}. This is the typical value for Fe(II)-HS state. This indicates that the SCO phenomenon does not occur from 78 K to room temperature. Q.S. value decreased in the order of NCS > NCSe > NCBH₃, as shown in Table 1.

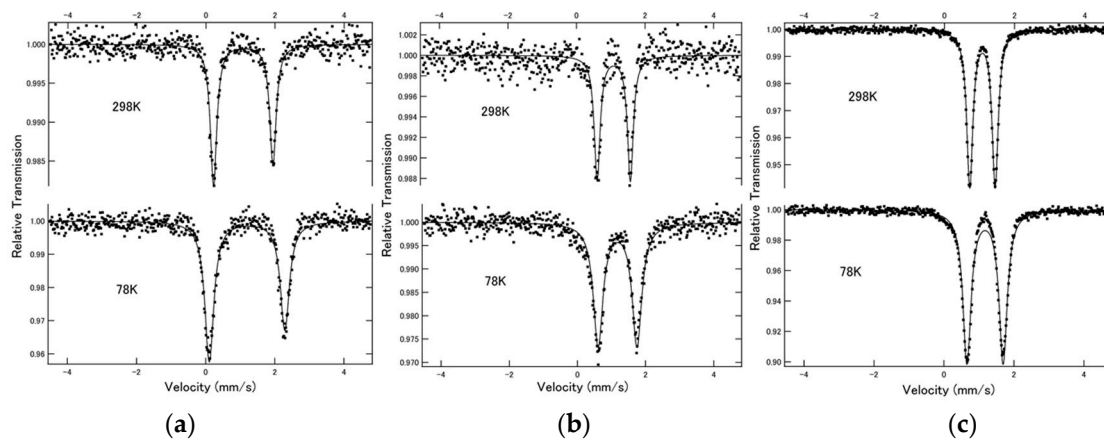


Figure 1. ^{57}Fe Mössbauer spectra of (a) **1**; (b) **2**; and (c) **3**.

Table 1. Mössbauer parameters for complexes **1**, **2**, and **3**.

Complex	T/K	I.S./mm·s ^{−1}	Q.S./mm·s ^{−1}	Γ /mm·s ^{−1}	Relative Area/%
1	298	0.95	1.72	0.23	100
	78	1.12	2.18	0.32	100
2	298	0.95	0.97	0.21	100
	78	1.04	1.14	0.34	100
3	298	0.95	0.72	0.21	100
	78	1.04	1.03	0.28	100

2.2. Magnetic Susceptibility

Figure 2 shows the magnetic susceptibilities of all complexes obtained on a SQUID magnetometer. The values of $\chi_{\text{M}}T$ of complexes **1**, **2**, and **3** are nearly constant (ca. 3.5 cm³·K·mol^{−1}). These values reveal that irons are in Fe(II)-HS state. This suggests that all complexes do not show the SCO phenomenon, although slight possibility of HS form quenching remains.

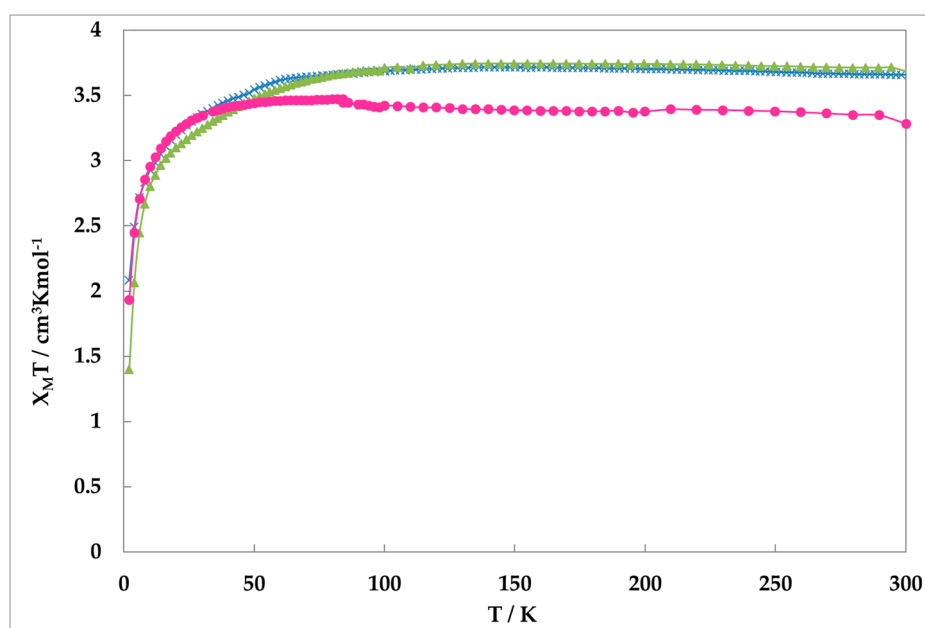


Figure 2. Magnetic susceptibility of **1** (red circle), **2** (green triangle), and **3** (blue cross).

2.3. Crystal Structure

The single crystal of $[\text{Fe}(\text{NCS})_2(\text{bpanth})_2]_n$ was obtained by diffusion method. Table 2 shows crystallographic data for complex **1** at 173 K. Figure 3a shows the Oak Ridge Thermal-Ellipsoid Plot Program (ORTEP) drawing and Figure 3b depicts the packing view of complex **1**. Guest molecule was not observed.

Table 2. Crystallographic data for complex **1**.

Complex	1
Formula	$\text{FeC}_{50}\text{H}_{32}\text{N}_6\text{S}_2$
$M/\text{g}\cdot\text{mol}^{-1}$	836.78
Crystal system	orthorhombic
Space group	Ibam
$a/\text{\AA}$	9.6020(7)
$b/\text{\AA}$	18.9796(14)
$c/\text{\AA}$	23.8123(18)
$\alpha/^\circ$	90
$\beta/^\circ$	90
$\gamma/^\circ$	90
$V/\text{\AA}^3$	4339.6(6)
Z	4
T/K	173.0(2)
μ/mm^{-1}	0.485
$\rho_{\text{calcd}} (\text{g}\cdot\text{cm}^{-3})$	1.286
R	0.0711
wR	0.1786
Goodness of fit	0.907

The iron of complex **1** is coordinated by bpanth in the equatorial plane, and by NCS in the axial position. The bond length of Fe–N (NCS) is 2.110(3) Å, and that of Fe–N (bpanth) is 2.246(3) Å. In general, the distance of Fe–N for octahedral complex in Fe(II)-HS is ca. 2.2 Å. These values suggest that the iron of this complex takes the HS state at 173 K. This result corresponds to the results of

Mössbauer spectroscopy and magnetic measurement. Figure 3b shows the packing view of the interpenetrated structure. 2D grids are interpenetrated to each other.

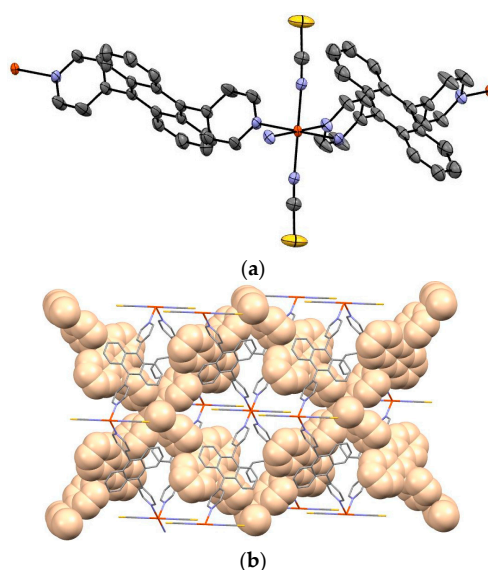


Figure 3. The ORTEP drawing (a) and the packing view (b) of complex 1.

2.4. Powder X-ray Diffraction (PXRD) Pattern

Figure 4 shows the PXRD patterns of complexes 1, 2, and 3. The complexes are obtained from EtOH–dichloromethane solution as well as water–dichloromethane solution. The pattern of the sample obtained from EtOH–dichloromethane solution is similar to that from water–dichloromethane solution in each complex, suggesting no effect of solvent in the crystal structure. The simulation pattern using single crystal data is almost the same as the experimental pattern of 1, suggesting the same structure between single crystal and the powder sample. However, a small amount of the other crystal was also suggested.

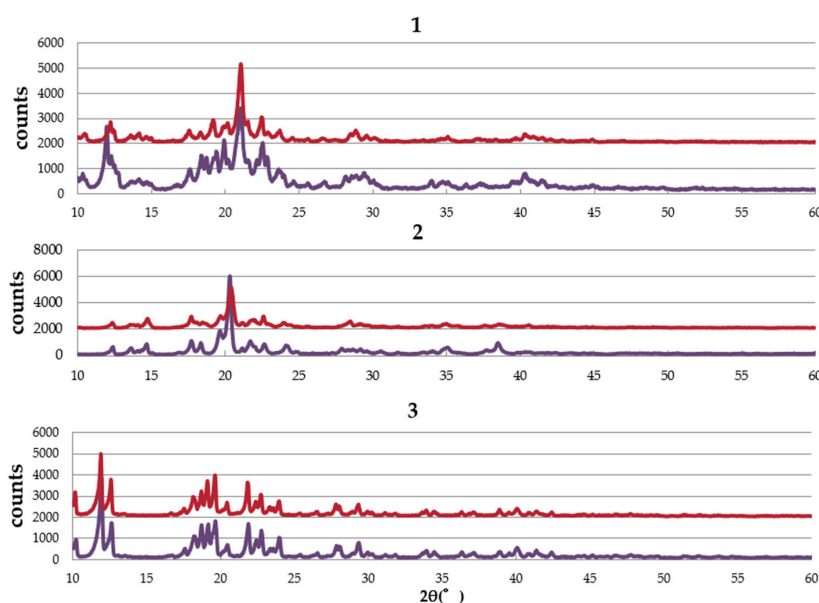


Figure 4. The powder X-ray diffraction (PXRD) patterns of 1, 2, and 3. Red and purple show the pattern of the crystals from EtOH–dichloromethane solution and water–dichloromethane solution, respectively.

3. Discussion

The measurements of the ^{57}Fe Mössbauer spectroscopy and magnetic susceptibility suggest that all complexes **1**, **2**, and **3** do not show the SCO phenomenon and take Fe(II)-HS state from 5 to 300 K. The obtained single crystal of complex **1** was analyzed by XRD, and the structure was revealed. Figure 5 illustrates the local structure around the iron atom. It can be easily seen that the planes of opposite pyridine rings are parallel to each other. As mentioned in the introduction, an earlier report [7,8] stated that complexes of this type do not undergo SCO. The present result corresponds to this report. Figure 5 shows why: In order for the iron atom to become LS, the ligands must approach the iron. In this conformation, this would cause hydrogen atoms of neighboring rings to come unreasonably close to each other.

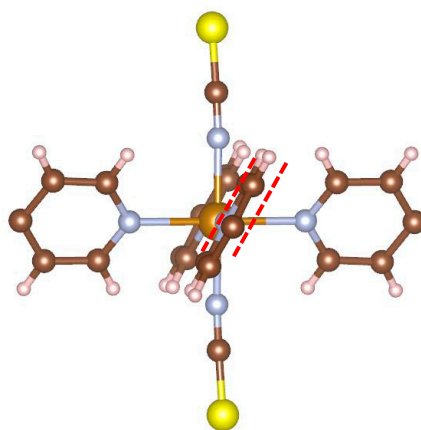


Figure 5. The local structure around the iron of complex **1**. Coordinated pyridine planes are parallel.

Figure 3b demonstrates the packing view of interpenetrated structure by 2D grids. It is suggested that this complex has intermolecular interactions. Figure 6 displays the focus picture of coordinated bridging ligand and neighboring bpanth of the other 2D grid. The pyridine of the upper ligand and the neighboring anthracene are orthogonal to each other. The distance between carbon atom and hydrogen atom (shown using a pink line) is 2.760(6) Å. This value is shorter than the sum (2.900 Å) of van der Waals radius for carbon and hydrogen atoms, and the C–H...C angle is 164.8(3) deg. This is the evidence that complex **1** has the CH– π interactions in the assembled structure. In this manner, this complex has the interpenetrated structure supported by the stabilization of CH– π interaction. Consequently, the coordinated pyridines facing each other are forced to become parallel, which is an unstable local structure.

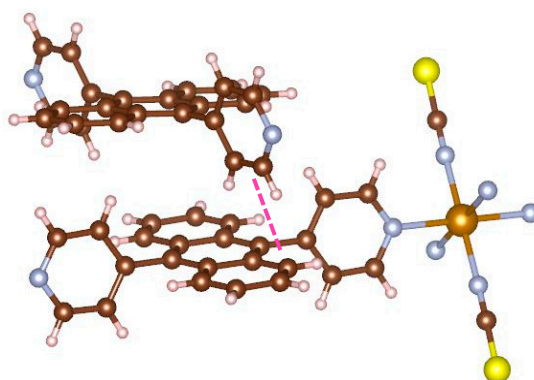


Figure 6. CH– π interaction between 2D grids.

Therefore, intermolecular interactions such as CH- π may prevent SCO phenomenon in the assembled complex, because such interactions affect the assembled structure and local structure around the iron atom. When an assembled complex has more flexible ligand or structure, it will have a possibility of showing the SCO phenomenon, because both the intermolecular interaction and the stability of the local structure around the iron atom do not need to compete.

4. Materials and Methods

4.1. Synthesis of Ligand and Complexes

4.1.1. Ligand

9,10-bis(4-pyridyl)anthracene (bpanth) was obtained by Suzuki–Miyaura cross-coupling reaction using 4-pyridyl boronic acid (18 mmol) and 9,10-dibromoanthracene (4 mmol) in toluene (60 mL) and water (60 mL). 1,1'-bis[(diphenylphosphino)ferrocene]dichloropalladium (1.2 mmol) as catalyst and Na_2CO_3 (20 mmol) as base were used in this reaction. The mixture was refluxed for 96 h under inactive gas atmosphere. The product was purified by column chromatography using alumina as the stationary phase and toluene as eluent. The alumina was deactivated by adding water (10 volume % to alumina), and then it was recrystallized from toluene. The bpanth was obtained as yellow crystal (yield: 72%) and identified by $^1\text{H-NMR}$ and elemental analysis. Anal. calcd. for $\text{C}_{24}\text{H}_{16}\text{N}_2$: C, 86.64%; H, 4.81%; N, 8.42%. Found for bpanth: C, 86.82%; H, 4.86%; N, 8.32%. $^1\text{H-NMR}$ (CDCl_3): δ 7.39 (q, 2H anthH $_{1,4}$), 7.44 (d, 2H, anthH $_{2,3}$), 7.60 (q, 2H PyH $_{\beta}$), 8.87 (d, 2H PyH $_{\alpha}$) ppm.

4.1.2. Complexes

Powder Complex of $[\text{Fe}(\text{NCX})_2(\text{bpanth})_2]_n$ (X = S (1), Se (2), BH_3 (3))

$\text{FeSO}_4 \cdot 7\text{H}_2\text{O}$ (0.2 mmol), RNCX salt (0.4 mmol: R = K, X = S; R = K, X = Se; R = Na, X = BH_3) and ascorbic acid were dissolved in degassed water (15 mL). The bpanth (0.4 mmol) in dichloromethane (15 mL) and the water solution were mixed directly and were stirred for 30 min. Yellow powder in the X = S case (yield: 92%) and in the X = Se case (yield: 89%) and yellowish white powder in the X = BH_3 case (yield: 66%) were obtained. Three products were identified by elemental analysis. Anal. calcd. for $\text{C}_{50}\text{H}_{32}\text{N}_6\text{S}_2\text{Fe} \cdot 0.8(\text{C}_2\text{H}_5\text{OH})$ (for single crystals below using EtOH as solvent): C, 70.93%; H, 4.25%; N, 9.62%. Found for $[\text{Fe}(\text{bpanth})_2(\text{NCS})_2 \cdot 0.8(\text{C}_2\text{H}_5\text{OH})]_n$: C, 70.64%; H, 3.96%; N, 10.05%. Anal. calcd. for $\text{C}_{50}\text{H}_{32}\text{N}_6\text{Se}_2\text{Fe}$: C, 64.53%; H, 3.47%; N, 9.03%. Found for $[\text{Fe}(\text{bpanth})_2(\text{NCSe})_2]_n$: C, 64.71%; H, 3.16%; N, 8.92%. Anal. calcd. for $\text{C}_{50}\text{H}_{38}\text{N}_6\text{B}_2\text{Fe}$: C, 75.03%; H, 4.79%; N, 10.50%. Found for $[\text{Fe}(\text{bpanth})_2(\text{NCBH}_3)_2]_n$: C, 73.10%; H, 4.53%; N, 10.07%.

Single Crystal of $[\text{Fe}(\text{NCS})_2(\text{bpanth})_2]_n$

$\text{FeSO}_4 \cdot 7\text{H}_2\text{O}$ (0.2 mmol) and ascorbic acid were dissolved in ethanol (7 mL) and stirred for 10 min. This solution was added to a solution of KNCS salt (0.4 mmol) in ethanol (7 mL) and was stirred for 10 min. This turbid solution was filtered, and clear solution was obtained. The clear solution was put in the bottom of a Schlenk flask. Mixed solvent of ethanol (15 mL) and dichloromethane (15 mL) was carefully added in the flask as middle layer. The bpanth (0.4 mmol) in dichloromethane (15 mL) was added as upper layer. The yellow single crystal was obtained and analyzed by single-crystal X-ray diffraction. CCDC 1573711 contains the supplementary crystallographic data for this paper (see Supplementary Materials). These data can be obtained free of charge via <http://www.ccdc.cam.ac.uk/conts/retrieving.html>.

4.2. Instrumental Analysis

4.2.1. ^{57}Fe Mössbauer Spectroscopy

^{57}Fe Mössbauer spectra were obtained for both samples from water–dichloromethane solution and EtOH–dichloromethane solution at 78, 298 K with a ^{57}Co (Rh) radiation source moving in constant acceleration mode on Wissel MB-500 (Wissenschaftliche Elektronik GmbH, Starnberg, Germany). The samples were cooled from 298 to 78 K for about 1 h. The 78 K was controlled during the measurement. The Mössbauer parameters were obtained by least-squares fitting to Lorentzian peaks. The spectra were calibrated by the six lines of $\alpha\text{-Fe}$, the center of which was taken as zero isomer shift. The samples from water–dichloromethane solution and EtOH–dichloromethane solution did not show a significant difference in each complex.

4.2.2. Magnetic Susceptibility Measurement

Magnetic susceptibility measurement was performed for the samples obtained from water–dichloromethane solution on a Quantum Design MPMS-5S SQUID apparatus (Quantum Design, Inc., San Diego, CA, USA). Magnetic field was 1000 Oe. The data of **1** were obtained for cooling mode at scan rate of 10 K/min from 300 to 200 K, 5 K/min from 200 to 100 K, and 2 K/min from 100 to 2 K. The data of **2** were obtained for heating mode at scan rate of 2 K/min from 300 to 2 K after the cooling from 300 to 2 K at the rate of 10 K/min. The data of **3** were obtained for cooling mode at scan rate of 5 K/min from 300 to 100 K, and 2 K/min from 100 to 2 K. The solvate molecules are not included in the calculation of molecular weight.

4.2.3. Powder X-ray Diffraction Pattern

Powder X-ray diffraction (PXRD) patterns were measured on RIGAKU RINT-2000 using $\text{Cu K}\alpha$ radiation (Rigaku Corp., Akishima, Japan). Scan rate was 2 degrees/min, step was 0.02 degrees, and scan region of 2θ was from 10 to 60 degrees for complexes **1**, **2**, and **3**. All measurements were performed at room temperature under air condition.

5. Conclusions

We synthesized three assembled complexes $[\text{Fe}(\text{NCX})_2(\text{bpanth})_2]_n$ ($X = \text{S}, \text{Se}, \text{BH}_3$; $\text{bpanth} = 9,10\text{-bis}(4\text{-pyridyl})\text{anthracene}$). ^{57}Fe Mössbauer spectroscopic measurement and magnetic susceptibility measurement revealed that the spin crossover phenomenon does not occur, and it remains in the Fe(II)-HS state. X-ray structural analysis suggested that complex **1** has the parallel-type local structure around the iron atom and there is CH– π interactions between 2D grids in interpenetrated structure. This overall structure is supported by the stabilization of CH– π interaction. However, it causes the formation of unstable parallel-type local structure which takes Fe(II)-HS state. Intermolecular interactions such as CH– π can prevent SCO phenomenon in assembled complex, because such interactions affect the assembled structure and local structure around the iron atom. When an assembled complex has more flexible ligand or structure, it has a possibility of showing the SCO phenomenon. We need to reveal the structures for other complexes and the effect to SCO from the point of interaction.

Supplementary Materials: The following are available online at www.mdpi.com/2304-6740/5/3/61/s1. Cif and cif-checked files.

Acknowledgments: We thank Inoue and members of Solid Material Chemistry Research Group, Hiroshima University for supporting magnetic susceptibility measurement and PXRD analysis. We also thank Mouri, the Natural Science Center for Basic Research and Development, Hiroshima University for the measurement of elemental analysis. We would like to thank Wiseman Chisale Bekelesi (MSc), Hiroshima University, for proofreading of English.

Author Contributions: Saki Iwai was involved in all stages of the work, including planning, conducting experiments, analyzing the data; Keisuke Yoshinami was involved in the discussion of the results and work

planning; Satoru Nakashima acted as the supervisor and helped the data analysis and work planning; and all the authors wrote the paper and contributed to the revision of the paper.

Conflicts of Interest: The authors declare no conflict of interest.

References

1. Gütllich, P.; Bill, E.; Trautwein, A.L. *Mössbauer Spectroscopy and Transition Metal Chemistry*; Springer: Berlin/Heidelberg, Germany, 2011; pp. 391–476, ISBN 978-3-540-88427-9.
2. Real, J.A.; André, E.; Muñoz, M.C.; Julve, M.; Granier, T.; Bousseksou, A.; Varret, F. Spin crossover in a catenane supramolecular system. *Science* **1995**, *268*, 265–267. [[CrossRef](#)] [[PubMed](#)]
3. Halder, G.J.; Kepert, C.J.; Moubaraki, B.; Murray, K.S.; Cashion, J.D. Guest-Dependent Spin Crossover in a Nanoporous Molecular Framework Material. *Science* **2002**, *298*, 1762–1765. [[CrossRef](#)] [[PubMed](#)]
4. Banerjee, H.; Chakraborty, S.; Saha-Dasgupta, T. Design and Control of Cooperativity in Spin-Crossover in Metal-Organic Complexes: A Theoretical Overview. *Inorganics* **2017**, *5*, 47. [[CrossRef](#)]
5. Morita, S.; Nakashima, S.; Yamada, K.; Inoue, K. Occurrence of the Spin-crossover Phenomenon of Assembled complexes, $\text{Fe}(\text{NCX})_2(\text{bpa})_2$ ($\text{X} = \text{S}, \text{BH}_3$; $\text{bpa} = 1,2\text{-bis}(4\text{-pyridyl})\text{ethane}$) by Enclathrating Organic Guest Molecule. *Chem. Lett.* **2006**, *35*, 1042–1043. [[CrossRef](#)]
6. Atsuchi, M.; Higashikawa, H.; Yoshida, Y.; Nakashima, S.; Inoue, K. Novel 2D Interpenetrated Structure and Occurrence of the Spin-crossover Phenomena of Assembled complexes, $\text{Fe}(\text{NCX})_2(\text{bpp})_2$ ($\text{X} = \text{S}, \text{Se}, \text{BH}_3$; $\text{bpp} = 1,3\text{-bis}(4\text{-pyridyl})\text{propane}$). *Chem. Lett.* **2007**, *36*, 1064–1065. [[CrossRef](#)]
7. Kaneko, M.; Tokinobu, S.; Nakashima, S. Density Functional Study on Spin-crossover Phenomena of Assembled Complexes, $[\text{Fe}(\text{NCX})_2(\text{bpa})_2]_n$ ($\text{X} = \text{S}, \text{Se}, \text{BH}_3$; $\text{bpa} = 1,2\text{-bis}(4\text{-pyridyl})\text{ethane}$). *Chem. Lett.* **2013**, *42*, 1432–1434. [[CrossRef](#)]
8. Kaneko, M.; Nakashima, S. Computational Study on Thermal Spin-Crossover Behavior for Coordination Polymers Possessing *trans*- $[\text{Fe}(\text{NCS})_2(\text{pyridine})_4]$ Unit. *Bull. Chem. Soc. Jpn.* **2015**, *88*, 1164–1170. [[CrossRef](#)]
9. Wu, X.-R.; Shi, H.-Y.; Wei, R.-J.; Li, J.; Zheng, L.-S.; Tao, J. Coligand and Solvent Effects on the Architectures and Spin-Crossover Properties of (4,4)-Connected Iron(II) Coordination Polymers. *Inorg. Chem.* **2015**, *54*, 3773–3780. [[CrossRef](#)] [[PubMed](#)]
10. Yoshinami, K.; Kaneko, M.; Yasuhara, H.; Nakashima, S. Effect of methyl substituent on the spin state of iron(II) assembled complex using 1,4-bis(4-pyridyl)benzene. *Radioisotopes* **2017**, in press.
11. Biradha, K.; Fujita, N. 2D and 1D Coordination Polymers with the Ability for Inclusion of Guest Molecules: Nitrobenzene, Benzene, Alkoxysilanes. *J. Incl. Phenom. Macrocycl. Chem.* **2001**, *49*, 201–208. [[CrossRef](#)]
12. Marin, G.; Andruh, M.; Madalan, A.M.; Blake, A.J.; Wilson, C.; Champness, N.R.; Schröder, M. Structural Diversity in Metal–Organic Frameworks Derived from Binuclear Alkoxo-Bridged Copper(II) Nodes and Pyridyl Linkers. *Cryst. Growth Des.* **2009**, *8*, 964–975. [[CrossRef](#)]



© 2017 by the authors. Licensee MDPI, Basel, Switzerland. This article is an open access article distributed under the terms and conditions of the Creative Commons Attribution (CC BY) license (<http://creativecommons.org/licenses/by/4.0/>).